Research Article Vol. 28, No. 7 / 30 March 2020 / Optics Express 9677
Optics EXPRESS

Electromagnetically induced transparency of interacting Rydberg atoms with two-body dephasing

DONG YAN,[1,2,*] BINBIN WANG,[1] ZHENGYANG BAI,[2,3] AND WEIBIN LI[2]

[1] School of Science and Key Laboratory of Materials Design and Quantum Simulation, Changchun University, Changchun 130022, China
[2] School of Physics and Astronomy, University of Nottingham, Nottingham, NG7 2RD, United Kingdom
[3] State Key Laboratory of Precision Spectroscopy, East China Normal University, Shanghai 200062, China
[*] ydbest@126.com

Abstract: We study electromagnetically induced transparency in a three-level ladder type configuration in ultracold atomic gases, where the upper level is an electronically highly excited Rydberg state. An effective distance dependent two-body dephasing can be induced in a regime where dipole-dipoles interaction couple nearly degenerate Rydberg pair states. We show that strong two-body dephasing can enhance the excitation blockade of neighboring Rydberg atoms. Due to the dissipative blockade, transmission of the probe light is reduced drastically by the two-body dephasing in the transparent window. The reduction of transmission is accompanied by a strong photon-photon anti-bunching. Around the Autler-Townes doublets, the photon bunching is amplified by the two-body dephasing, while transmission is largely unaffected. Besides relevant to the ongoing Rydberg atom studies, our study moreover provides a setting to explore and understand two-body dephasing dynamics in many-body systems.

1. Introduction

Electromagnetically induced transparency (EIT) [1–3] plays a pivotal role in quantum and nonlinear optics [4–8] and has been investigated intensively in the past two decades [9–12]. Recently there has been a growing interest in the study of EIT using electronically highly excited (Rydberg) states with principal quantum number $n \gg 1$. Rydberg atoms have long life times ($\sim n^3$) and strong two-body interactions (e. g. van der Waals interaction strength $\sim n^{11}$). The distance dependent interaction can suppress multiple Rydberg excitation of nearby atoms, giving rise to the so-called Rydberg excitation blockade. By mapping the Rydberg atom interaction to light fields through EIT [13], strong and long-range interactions between individual photons can be achieved. This permits to study nonlinear quantum optics at the few-photon level [14,15] and find quantum information applications [16] to create single photon sources [17–19], filters [13,20], subtractors [21,22], transistors [23,24], switches [25,26], and gates [27,28].

On the other hand, dephasing and decay of Rydberg atoms are unavoidable due to, e.g., atomic motions and finite laser linewidth [29]. In the study of long time dynamics, it has been shown that dissipation of individual atoms competes against the Rydberg interaction as well as laser-atom coupling. The interplay leads to interesting driven-dissipative many-body dynamics, such as glassy behaviors induced by single atom dephasing [30], bistability and metastability [31,32], Mott-superfluid phase transition [33], emergence of antiferromagnetic phases [34], dissipation controlled excitation statistics [35], and dissipation induced blockade and anti-blockade [36].

#389247 https://doi.org/10.1364/OE.389247
Journal © 2020 Received 27 Jan 2020; revised 11 Mar 2020; accepted 12 Mar 2020; published 19 Mar 2020

Optics EXPRESS

Nonetheless, collective dissipative processes emerge in dense atomic gases, typically through two-body dipolar couplings [37,38], leading to sub- and super-radiance.

In this work, we study Rydberg-EIT in a setting where both van der Waals interactions and two-body dephasing are present. The latter could be induced by dipolar couplings between different Rydberg pair states when they are nearly degenerate [31,39–52]. We derive a master equation in which van der Waals (vdW) interactions and two-body dephasing (TBD) are both present in a target Rydberg state. By directly diagonalizing the master equation of small systems and applying superatom (SA) method for large systems [53], we study stationary properties of the Rydberg-EIT due to the interplay between the coherent and incoherent two-body processes. A key finding is that the blockade radius is enlarged by the two-body dephasing, which modifies transmission and photon-photon correlation of the probe field.

The structure of the paper is as follows. In Sec. 2, the many-body Hamiltonian and master equation that is capable to capture the two-body processes is introduced. In Sec. 3, the modification of the blockade radius by the two-body dephasing is discussed. We achieve this by numerically solving the master equation for two atoms, and analyze an effective Hamiltonian. In Sec. 4, we solve the light propagation and atomic dynamics through the Heisenberg-Langevin approach. We identify parameters where the transmission of the probe light is affected by the TBD. Photon-photon correlations are drastically modified by the TBD in the transparent window and around Autler-Townes splitting. The conclusion is given in Sec. 5.

2. Many-atom Hamiltonian and the master equation

We consider a cold gas of N Rb atoms, which are described by a three-level ladder type configuration with a long-lived ground state $|g\rangle$, a low-lying excited state $|e\rangle$ with decay rate γ_e, and a highly excited Rydberg state $|d\rangle$. The level scheme is shown in Fig. 1(a). Specifically these states are given by $|g\rangle = |5S\rangle$, $|e\rangle = |5P\rangle$ and $|d\rangle = |nD\rangle$. The upper transition $|e\rangle \rightarrow |d\rangle$ is driven by a classical control field with Rabi frequency Ω_d and detuning Δ_d. The lower transition $|g\rangle \rightarrow |e\rangle$ is coupled by a weak laser field, whose electric field operator and detuning is given by $\hat{\mathcal{E}}_p$ and Δ_p, respectively. Long-range van der Waals (vdW) interactions $V_{jk} = C_6/R_{jk}^6$ between two atoms located at $\mathbf{r}_j$ and $\mathbf{r}_k$ (C_6 and $R_{jk} = |\mathbf{r}_j - \mathbf{r}_k|$ the dispersion coefficient and atomic distance) shift Rydberg states out of resonance, and hence affect transmission of the probe light [54–63]. The Hamiltonian of the system reads ($\hbar \equiv 1$)

$$\hat{H} = \hat{H}_0 + \hat{V}_d(R), \tag{1}$$

where $\hat{H}_0 = \sum_{j=1}^{N}[\Delta_p \hat{\sigma}_{ee}^j + (\Delta_p + \Delta_d)\hat{\sigma}_{dd}^j] + [\hat{\Omega}_p \hat{\sigma}_{eg}^j + \Omega_d \hat{\sigma}_{ed}^j + \text{H.c}]$ describes the atom-light coupling. We have defined the Rabi frequency operator $\hat{\Omega}_p = g\hat{\mathcal{E}}_p$ with g the single atom coupling constant [29]. $\hat{V}_d(R) = \sum_{j>k} V_{jk}\hat{\sigma}_{dd}^j \hat{\sigma}_{dd}^k$ is the vdW interaction between Rydberg atoms. Here $\hat{\sigma}_{mn}^j = |m\rangle_j\langle n|$ is the transition operator of the j-th atom.

A pair of atoms in the Rydberg $|d\rangle$ state can couple to other pairing states of similar energies via dipole-dipole interactions, due to the small quantum defects in Rydberg $|d\rangle$ state as well as the presence of Föster resonances. To avoid treat these background states explicitly, we will assume atoms in the background states decay rapidly to the $|d\rangle$ state. This allows us to adiabatically eliminate the molecular states, which leads to an effective, two-body dephasing in the $|d\rangle$ state (see Appendix for derivation). Further taking into account of other decay processes, dynamics of

Optics EXPRESS

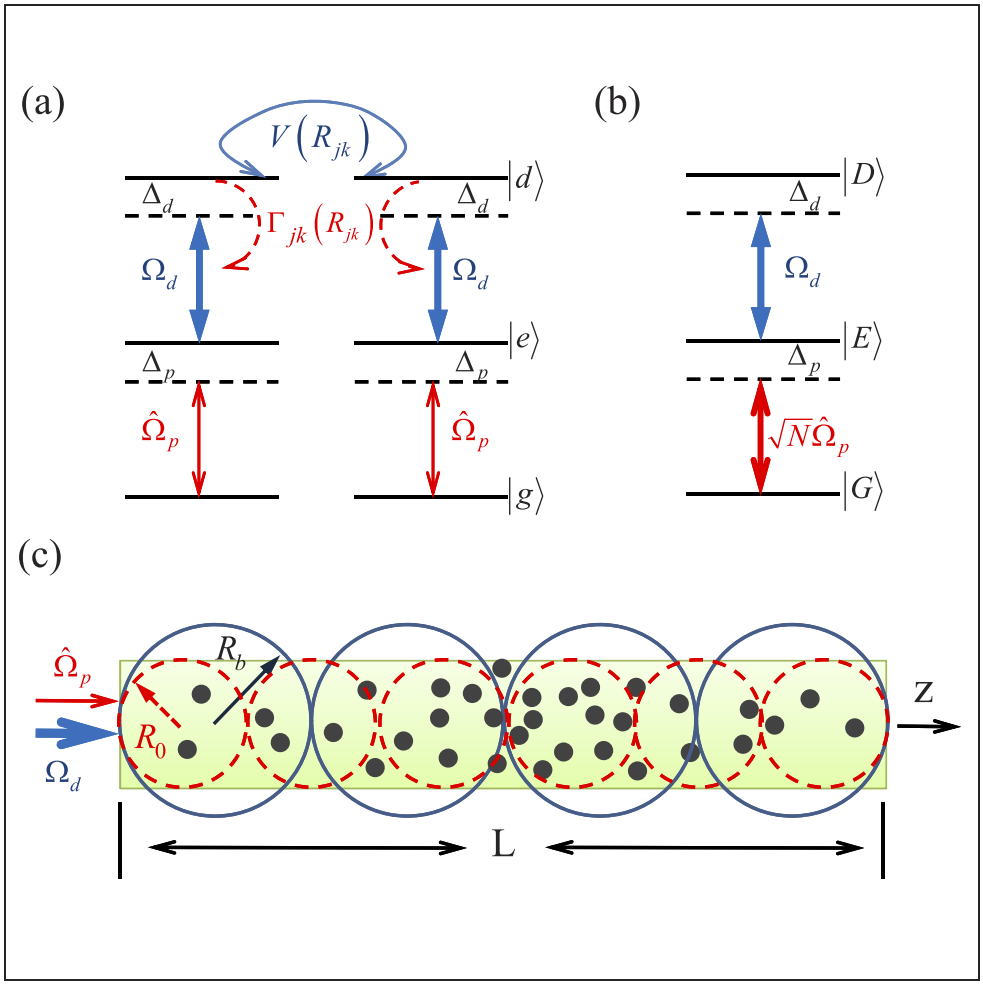

Fig. 1. (**a**) Atomic levels. A weak probe field (Rabi frequency operator $\hat{\Omega}_p$ and detuning Δ_p) and a classical coupling field (Rabi frequency Ω_d and detuning Δ_d) couple the ground state $|g\rangle$, intermediate state $|e\rangle$ and Rydberg state $|d\rangle$, respectively. V_{jk} and Γ_{jk} are long-range van der Waals interaction and two-body dephasing. (**b**) A superatom is composed of three collective state $|G\rangle$, $|E\rangle$ and $|D\rangle$. The collective coupling between states $|G\rangle$ and $|E\rangle$ is enhanced by $\sqrt{N}$. (**c**) SAs with (blue solid line) and without (red dashed line) TBD in a quasi one-dimensional atomic ensemble (length L). The number of SAs decreases as the size of SAs increases.

Optics EXPRESS

the many-atom system is governed by the following master equation

$$\begin{aligned}\dot{\varrho} = &-i[\hat{H}, \varrho] + 2\gamma_e \sum_j \left(\hat{\sigma}^j_{ge}\varrho\hat{\sigma}^j_{eg} - \frac{1}{2}\{\varrho, \hat{\sigma}^j_{eg}\hat{\sigma}^j_{ge}\}\right) \\ &+ 2\gamma_d \sum_j \left(\hat{\sigma}^j_{dd}\varrho\hat{\sigma}^j_{dd} - \frac{1}{2}\{\varrho, \hat{\sigma}^j_{dd}\}\right) \\ &+ \sum_{j>k} \Gamma_{jk}\left(\hat{\sigma}^j_{dd}\hat{\sigma}^k_{dd}\varrho\hat{\sigma}^k_{dd}\hat{\sigma}^j_{dd} - \frac{1}{2}\{\varrho, \hat{\sigma}^k_{dd}\hat{\sigma}^j_{dd}\}\right),\end{aligned} \tag{2}$$

where γ_d is single atom dephasing rate in state $|d\rangle$. $\Gamma_{jk} = \Gamma_6/R^6_{jk}$ is distance dependent two-body dephasing with Γ_6 being a coefficient characterizing the strength of the TBD.

3. Two-body dephasing enhanced blockade effect

In this section, we study effects caused by the two-body dephasing in a two-atom setting. We first calculate stationary states of two atoms by solving the master Eq. (2) numerically. Using the stationary state solution, we evaluate the two-body correlation

$$C(R_{12}) = \frac{\langle\hat{\sigma}^1_{dd}\hat{\sigma}^2_{dd}\rangle}{\langle\hat{\sigma}^1_{dd}\rangle\langle\hat{\sigma}^2_{dd}\rangle}. \tag{3}$$

Different values of $C(R)$ give different statistics of the system. $C(R)<1$ [$C(R)>$] corresponds to the anti-bunching (bunching) effect, where double Rydberg excitations are suppressed (enhanced). The anti-bunching is associated to a sub-Poissonian statistics in the excitation while bunching a super-Poissonian. In the special case $C(R) = 1$ Rydberg excitations are independent from each other which follows a Poissonian distribution.

Dependence of the correlation on the atomic separation is studied under the two-photon resonance ($\Delta_p + \Delta_d = 0$). Simultaneous excitations of the two atoms are prohibited at short distances, due to the vdW interaction and TBD. As a result, the correlation around $R \approx 0$ is negligible [see Fig. 2(a)]. The correlation increases rapidly at intermediate distances (around $R \sim R_0$), and saturates at 1 when $R \to \infty$. When the single photon detuning (i.e. Δ_p) is large, a maximum correlation is found at intermediate distances [see marked data points in Fig. 2(a)]. Focusing on the large detuning regime, we find that heights of the maximal correlation decreases but its location increases when the strength of the TBD increases, as shown in Fig. 2(b). Such result indicates that the TBD enhances the blockade effect. More specifically, we will show that the two-body dephasing can increase the blockade radius.

3.1. Blockade radius in the presence of TBD

Without TBD and for large single photon detuning, the blockade radius is $R_0 \simeq \sqrt[6]{C_6\,|\gamma_e + i\Delta_d|\,/\Omega_d^2}$, due to the competition between the linewidth in the Rydberg state and the vdW interaction [22,50,53,55,56,59,60,64–66]. Only one Rydberg atom can be excited in a volume determined by the blockade radius R_0 while multiple excitations are prevented by the vdW interaction.

When the TBD is present, the non-Hermitian Hamiltonian of the system is,

$$\hat{H}_{eff} = \hat{H}_0 + \sum_{j>k}\left(\frac{C_6}{R^6_{jk}} - i\frac{\Gamma_6}{2R^6_{jk}}\right)\hat{\sigma}^j_{dd}\hat{\sigma}^k_{dd}, \tag{4}$$

where the vdW interaction and TBD are grouped together. By treating the two terms as a complex interaction, and using the same argument as we derived R_0, a new characteristic radius R_b is

Optics EXPRESS

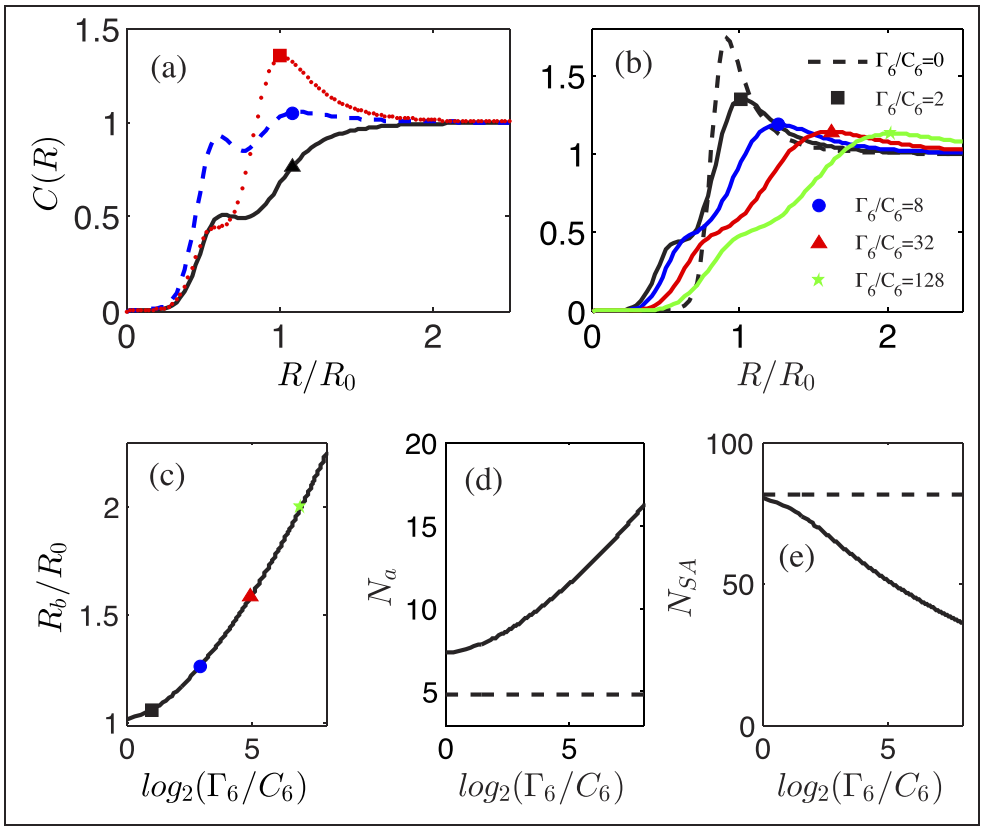

Fig. 2. (**a**) Correlation function $C(R)$ for $\Delta_d = -\Delta_p = -2\pi \times 0.3$ MHz (solid), $\Delta_d = -\Delta_p = -2\pi \times 2.0$ MHz (dashed) and $\Delta_d = -\Delta_p = -2\pi \times 4.0$ MHz (dotted). A maximum is found when the single photon detuning $|\Delta_p| = |\Delta_d|$) is large. Other parameters are $\Gamma_6 = 2C_6$ and $\Omega_p/2\pi = 0.5$ MHz. (**b**) Correlation function $C(R)$ with large single photon detuning $\Delta_d = -\Delta_p = -2\pi \times 4.0$ MHz. Increasing the TBD rate Γ_6, the maximal values reduce gradually. (**c**) R_b v.s. Γ_6. The location corresponding to the maximal value of the correlation function is marked [see Fig. 2(b)]. (**d**) Number N_a of atoms per superatom and (**e**) number N_{SA} of superatoms in the one-dimensional atomic ensemble. As the blockade radius increases with Γ_6, the volume of a superatom becomes larger. Fixing the length of the medium, the number of superatoms is reduced. Other parameters for panels (b-e) are $\Omega_d/2\pi = 2.0$ MHz, $\gamma_e/2\pi = 3.0$ MHz, $\gamma_d/2\pi = 10.0$ kHz, $C_6/2\pi = 140\,\text{GHz}\,\mu\text{m}^6$, and $L = 1.0$ mm.

obtained,

$$R_b \simeq \sqrt[6]{\left|1 - i\frac{\Gamma_6}{2C_6}\right|}R_0, \tag{5}$$

which depends on both the vdW interaction and TBD.

Especially this radius increases with the TBD rate Γ_6. In the strong dephasing limit $\Gamma_6 \gg C_6$, it is fully determined by the dephasing rate, $R_b \sim \sqrt[6]{\Gamma_6/2C_6}R_0$. Importantly the radius R_b is identical to the distance corresponding to the maximal correlation, as shown in Fig. 2(b) and (c). Such results are similar to the derivation of the blockade radius in conventional Rydberg-EIT [66]. Hence we will treat R_b as an effective blockade radius for this dissipative optical medium.

Optics EXPRESS

3.2. Enhancement of the blockade effect

As the blockade radius is increased by the TBD, the blockade effect is enhanced in a high density atomic gas. In a blockade volume, the atoms are essentially two-level atoms (in states $|g\rangle$ and $|e\rangle$). They behave as a superatom (SA) consisting of three collective states [50,53,59,60,64,65], i.e the collective ground state $|G\rangle = \left|g_1,\ldots,g_{N_a}\right\rangle$, singly excited state $|E\rangle = \sum_j \left|g_1,\ldots,e_j,\ldots,g_{N_a}\right\rangle/\sqrt{N_a}$ and $|D\rangle = \sum_j \left|g_1,\ldots,d_j,\ldots,g_{N_a}\right\rangle/\sqrt{N_a}$ [see Fig. 1(b)]. The number of the blocked atoms in the volume $V = 4\pi R_b^3/3$ of a superatom is given by $N_a = 4\pi\rho R_b^3/3$, where ρ is the density of the atomic gas. Hence the TBD increases the "mass" (i. e. the number of atoms) of a superatom [see Fig. 1(c) and Fig. 2(d)]. In the weak probe field limit, collective states containing two or more Rydberg excitations are prohibited from the dynamics due to the blockade.

In the one dimensional case, the number of superatoms $N_{SA} = L/R_b$ reduces as the blockade radius increases. However the number of atoms that are blocked $N_{\rm tot} = N_{SA}N_a = 4\pi L\rho R_b^2/3$ increases with increasing blockade radius. Therefore we obtain less superatoms, while the total number of blocked atoms (i.e. two-level atoms) is increased. These two-level atoms breaks the EIT condition and causes light scattering. As a result the transmission is reduced when the TBD rate is large.

4. Transmission and correlation of the probe light

In this section, we will study stationary properties of the weak probe light through the Heisenberg-Langevin approach. We will work in the continuous limit, which is valid when the atomic density is high. The one dimensional regime is realized when widths of light pulses are smaller than the blockade radius.

4.1. Heisenberg-Langevin equations

Using the superatom model and the master Eq. (2) we obtain Heisenberg-Langevin equations of light and atomic operators [53]

$$\begin{aligned}
\partial_t\hat{\mathcal{E}}_p(z) &= -c\partial_z\hat{\mathcal{E}}_p(z) + i\eta N\hat{\sigma}_{ge}(z),\\
\partial_t\hat{\sigma}_{ge}(z) &= -\left(i\Delta_p+\gamma_e\right)\hat{\sigma}_{ge}(z) - i\hat{\Omega}_p^{\dagger}(z) - i\Omega_d\hat{\sigma}_{gd}(z),\\
\partial_t\hat{\sigma}_{gd}(z) &= -i\left[\Delta+\hat{S}_V(z)-i\hat{S}_\Gamma(z)\right]\hat{\sigma}_{gd}(z)\\
&\quad -\gamma_d\hat{\sigma}_{gd}(z) - i\Omega_d\hat{\sigma}_{ge}(z),
\end{aligned} \tag{6}$$

where $\Delta = \Delta_p + \Delta_d$ is the two-photon detuning. $\hat{S}_V(z) = \int d^3z'\rho(z')\,C_6/|z-z'|^6\,\hat{\sigma}_{dd}(z')$ and $\hat{S}_\Gamma(z) = \int d^3z'\rho(z')\,\Gamma_6/2\,|z-z'|^6\,\hat{\sigma}_{dd}(z')$ denote the interaction energy and TBD rate, respectively. Both $\hat{S}_V$ and $\hat{S}_\Gamma$ are nonlocal in the sense that these quantities depend on the overall density $\rho(z)$ of the atomic gas and Rydberg state population.

Knowing the blockade radius, we solve the Heisenberg-Langevin equations of independent SAs in the steady state and obtain the Rydberg excitation projection operator [53],

$$\hat{\Sigma}_{DD}(z) = \frac{N_a\eta^2\hat{\mathcal{E}}_p^{\dagger}(z)\,\hat{\mathcal{E}}_p(z)\,\Omega_d^2}{N_a\eta^2\hat{\mathcal{E}}_p^{\dagger}(z)\,\hat{\mathcal{E}}_p(z)\,\Omega_d^2 + \left(\Omega_d^2-\Delta\Delta_p\right)^2 + \Delta^2\gamma_e^2}. \tag{7}$$

The polarizability of the probe field is conditioned on the projection,

$$\hat{P}(z) = \hat{\Sigma}_{DD}(z)\,P_2 + \left[1-\hat{\Sigma}_{DD}(z)\right]P_3 \tag{8}$$

Optics EXPRESS

where the polarizability becomes that of two-level atoms in a SA

$$P_2 = \frac{i\gamma_e}{\gamma_e + i\Delta_p} \tag{9}$$

and that of three-level atoms otherwise

$$P_3 = \frac{i\gamma_e}{\gamma_e + i\Delta_p + \frac{\Omega_d^2}{\gamma_d + i\Delta}}. \tag{10}$$

It is clearly that optical response of a SA depends on the Rydberg projection operator (7), i.e., SAs behave like a two-level, absorptive medium due to $\hat{\Sigma}_{DD}(z) = 1$.

The transmission of the probe light is captured by the probe light intensity $I_p(z) = \langle \hat{\mathcal{E}}_p^\dagger(z)\hat{\mathcal{E}}_p(z)\rangle$. In the steady state, the intensity $I_p(z)$ satisfies a first order differential equation,

$$\partial_z \langle \hat{\mathcal{E}}_p^\dagger(z)\hat{\mathcal{E}}_p(z)\rangle = -\kappa(z)\langle \mathrm{Im}[\hat{P}(z)]\hat{\mathcal{E}}_p^\dagger(z)\hat{\mathcal{E}}_p(z)\rangle, \tag{11}$$

where $\kappa(z) = \rho(z)\,\omega_p/(\epsilon_0 c\gamma_e)$ denotes the resonant absorption coefficient. Similarly we find the two-photon correlation function $g_p(z) = \langle \hat{\mathcal{E}}_p^{\dagger 2}(z)\hat{\mathcal{E}}_p^2(z)\rangle / \langle \hat{\mathcal{E}}_p^\dagger(z)\hat{\mathcal{E}}_p(z)\rangle^2$ obeys [53]

$$\partial_z g_p(z) = -\kappa(z)\mathrm{Im}[P_2 - P_3]\langle \hat{\Sigma}_{DD}(z)\rangle g_p(z). \tag{12}$$

The blockade radius is encoded in the correlation function of photon pairs, which decays with the rate proportional to the excitation probability $\langle \hat{\Sigma}_{DD}\rangle$ and absorption rate of a two-level atom when photon separation is smaller than the blockade radius.

To solve Eq. (6)–(12) the 1D atomic medium is divided into $N_{SA} = L/(2R_b)$ superatoms, and then we judge Rydberg excitation whether $\langle \hat{\Sigma}_{DD}(z)\rangle \to 1$ or $\langle \hat{\Sigma}_{DD}(z)\rangle \to 0$ in each SA one by one via a Monte Carlo sampling. This procedure is repeated many times in order to evaluate mean values.

4.2. Transmission of the probe field

The transmission of the probe field is characterized by the ratio of light intensities at the output and input, i.e. $\tilde{I}_p(L) = I_p(L)/I_p(0)$ with input values $I_p(0)$. Without vdW interactions or TBD, high transmission is obtained in the EIT window $|\Delta_p| \le |\Omega_d|^2/\gamma_e$ due to the formation of dark state polaritons [3]. The vdW interaction will reduce the transmission. When turning on the TBD, the transmission is further suppressed in the EIT window, see Fig. 3(a). Increasing the TBD strength Γ_6, the transmission $\tilde{I}_p(L)$ decreases gradually [Fig. 3(b)]. A weaker transmission indicates that there are more atoms prohibited from forming dark state polaritons [3]. This is consistent with the analysis in Sec. 3B.

Outside the EIT window ($|\Delta_p| > \Omega_d^2/\gamma_e$), the transmission first decreases with increasing detuning Δ_p. It arrives at the minimal transmission around the Autler-Townes splitting $\Delta_p = \pm\Omega_d$. In this region, the TBD is almost negligible [Fig. 3(a)]. Similar to the transmission of EIT in a Rydberg medium [53], the medium enters a linear absorption regimes, where neither vdW interactions nor TBD affects photon absorption dramatically.

In the following, we will focus on the transmission in the EIT window and explore how the TBD interplays with other parameters. We first calculate the transmission by varying atomic density and probe field Rabi frequency. To highlight effects due to the TBD, we calculate differences of the transmission with and without TBD, $\delta\tilde{I} = \tilde{I}_p(L) - \tilde{I}_p^0(L)$ where $\tilde{I}_p^0(L)$ denotes the light transmission when the TBD is turned off. The result is shown in Fig. 3(c). We find that stronger probe field (larger Ω_p) and higher atomic densities in general lead to more pronounced TBD effect. The "phase diagram" shown in Fig. 3(c) allows us to distinguish TBD dominated regions. To do so, we plot a phase boundary (dashed curve) when the difference $\delta\tilde{I} > 1\%$. Below

Optics EXPRESS

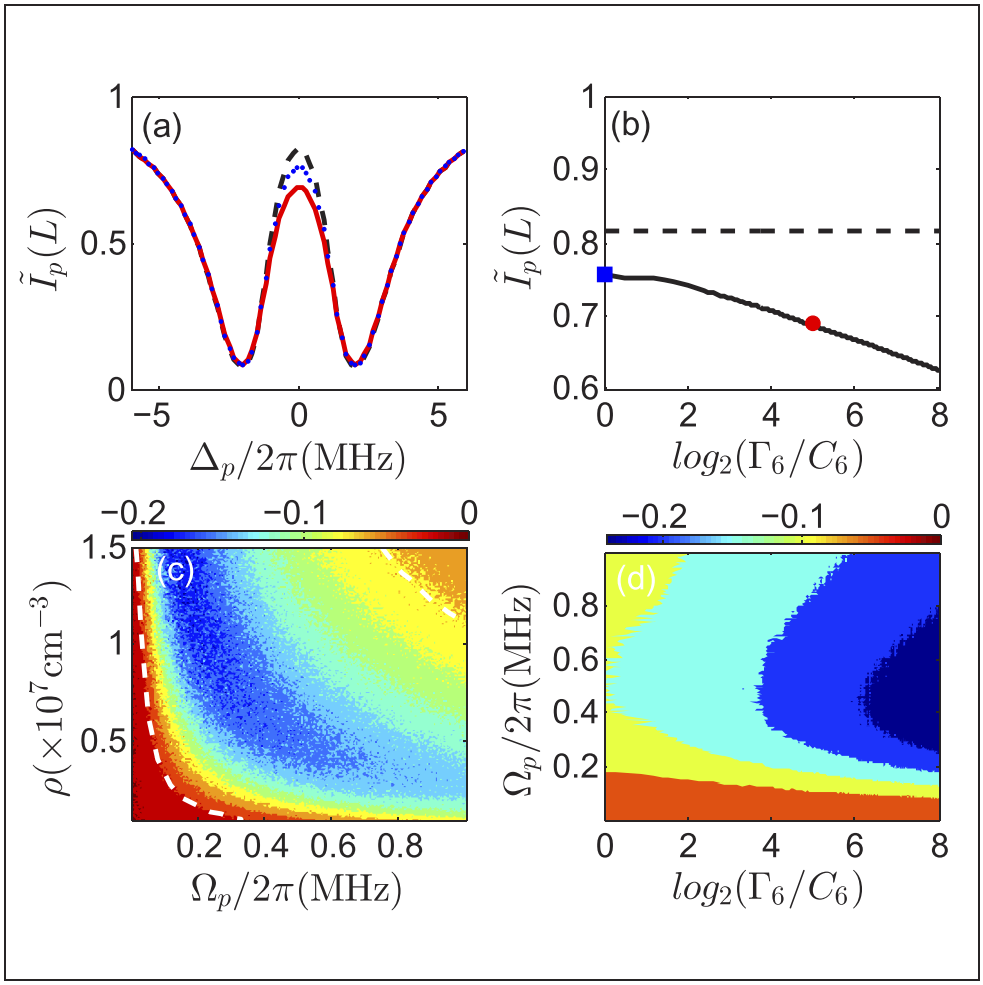

Fig. 3. (**a**) Transmission v.s. the detuning Δ_p for TBD rate $\Gamma_6 = 0$ (dashed), $\Gamma_6 = C_6$ (dotted) and $\Gamma_6 = 32C_6$ (solid). (**b**) Dependence of the transmission on the TBD rate Γ_6 at the EIT resonance. The square and circle denote values of the transmission in (a) when $\Gamma_6 = 0$ and when $\Gamma_6 = 32C_6$. (**c**) Diagram of the transmission as a function of Rabi frequency Ω_p and atomic density ρ. A TBD active region is found when $|\delta\tilde{I}_p(L)|>1\%$ (dashed line). The probe detuning $\Delta_p = 0$. (**d**) Diagram of the transmission as a function of TBD rate Γ_6 and Rabi frequency Ω_p. Increasing Γ_6 and Ω_p will reduce the transmission. The latter is caused by stronger blockade effect due to vdW density-density interactions. In panels (a), (b) and (d), the atomic density is $\rho = 0.5 \times 10^{11}$ mm^{-3}. Rabi frequency $\Omega_p(0)/2\pi = 0.3$ MHz in (a) and (b). $\Gamma_6 = 32C_6$ in panel (c). Other parameters are same with that of Fig. 2.

this curve the transmission is largely affected by the vdW interactions while above this curve, the atomic gas exhibits active TBD phase. Namely, the transmission is reduced significantly due to the TBD.

In Fig. 3(d), we show the transmission by varying both the Rabi frequency Ω_p and TBD rate Γ_6. Fixing Γ_6, the transmission decreases with increasing Ω_p. This results from the strong energy shift caused by the vdW interaction [22,53] . On the other hand, the transmission decreases with increasing Γ_6 if one fixes Ω_p, i.e. the EIT is dominantly affected by the TBD.

Optics EXPRESS

4.3. Photon-photon correlation

The photon-photon correlation function exhibits nontrivial dependence on the TBD. The normalized correlation function $\tilde{g}_p(L) = g_p(L)/g_p(0)$ at the exist of the medium is shown in Fig. 4(a). In the EIT window, the correlation $\tilde{g}_p(L)$ becomes smaller when we turn on the TBD. Increasing the TBD strength Γ_6, the correlation decrease [see Fig. 4(a) and Fig. 4(b)]. A smaller correlation indicates that anti-bunching becomes stronger. It is interesting to note that the transmission is large [Fig. 3(a)] in the EIT window.

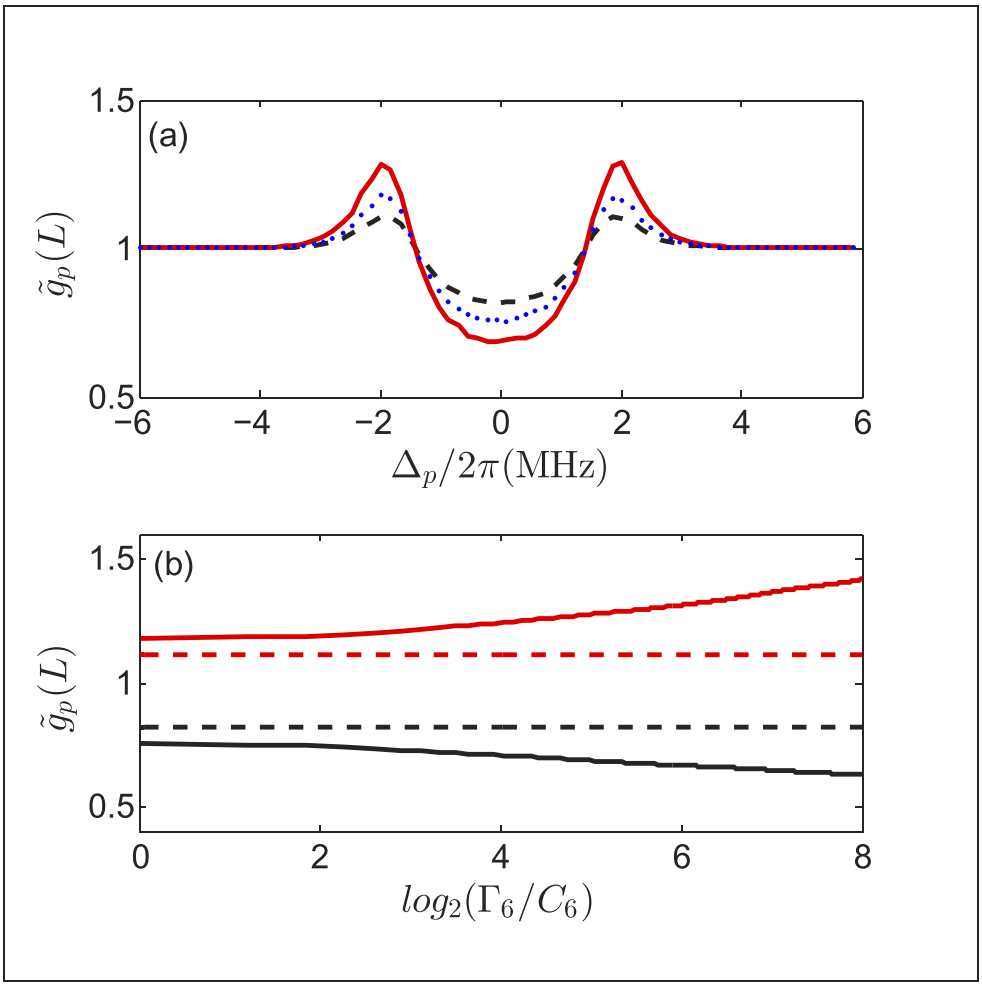

Fig. 4. (**a**) Second-order correlation function $\tilde{g}_p(L)$ versus the probe detuning $\Delta_p/2\pi$ for TBD rate $\Gamma_6 = 0$ (dashed), $\Gamma_6 = C_6$ (dotted) and $\Gamma_6 = 32C_6$ (solid). (**b**) Dependence of the second-order correlation function $\tilde{g}_p(L)$ on the TBD rate Γ_6 when $\Delta_p/2\pi = 0.0$ MHz (black solid) and $\Delta_p/2\pi = 2.0$ MHz (red solid). The dashed black curve ($\Delta_p/2\pi = 0.0$ MHz) and dashed red curve ($\Delta_p/2\pi = 2.0$ MHz) denote the TBD rate $\Gamma_6 = 0$. Other parameters are the same as in Fig. 2.

In contrast, the correlation $\tilde{g}_p(L)$ is enhanced by the TBD outside the EIT window. We obtain maximal correlations around the Autler-Townes doublet $\Delta_p \approx \pm\Omega_d$. Increasing Γ_6, the maximal value (bunching) is also increased [see Fig. 4(c)]. We shall point out that the transmission is the

Optics EXPRESS

smallest at the Autler-Townes doublet. It might become difficult to observe the TBD amplified bunching in this case, as the photon flux is low.

5. Conclusions

In summary, we have studied EIT in a one-dimensional gas of cold atoms involving highly excited Rydberg states. In this model, each pair of atoms does not only experience the long-range vdW interaction but also the nonlocal two-body dephasing. The TBD can enlarge the effective blockade radius. We demonstrate that in the EIT window, the TBD enhances the blockade effect, i.e. reducing the transmission and increasing photon-photon anti-bunching. Away from the EIT window, the transmission is hardly affected by the TBD. However, the photon bunching is amplified around the Autler-Townes doublet.

In the present work, we focused on stationary states of the probe light in a 1D setting. It is worth studying how the combination of TBD and vdW interactions will affect propagating of short light pulses, as well as transient dynamics [46,47]. In 2D and 3D, the angular dependence of the effective dephasing will affect light propagation and Rydberg excitation dynamics in atomic gases. We are exploring these physics based on the model studied in this work. Beyond cold Rydberg atom physics, our work is relevant to the study of many-body physics and open quantum systems. The master equation provides a setting to explore and understand many-body dissipative dynamics and equilibrium phases that is influenced by two-body dephasing.

Appendix: derivation of the two-body dephasing operator

We consider a pair of atoms in Rydberg $|d\rangle$ state couple to a different Rydberg state $|r\rangle$ through a molecular process. This is described by the Hamiltonian $H_t = H + H_m$, where H is the Hamiltonian given by Eq. (1), and the molecular Hamiltonian H_m describes the dipolar interaction between the Rydberg states,

$$\hat{H}_m = U(R_{12})(\hat{\sigma}^1_{dr}\hat{\sigma}^2_{dr} + \hat{\sigma}^1_{rd}\hat{\sigma}^2_{rd}), \tag{13}$$

with the dipolar interaction $U(R_{12}) = C_3/R_{12}^3$. Moreover the state $|r\rangle$ decays to the $|d\rangle$ through a single body spontaneous process. The dynamics is given by the master equation,

$$\begin{aligned}\dot{\hat{\rho}}_m &= -i[\hat{H}_m, \hat{\rho}_m] \\ &\quad + \gamma_r \sum_{j,k=1,2,j\neq k} \left(\hat{\sigma}^j_{dr}\hat{\rho}_m\hat{\sigma}^k_{rd} - \frac{1}{2}\{\hat{\rho}_m, \hat{\sigma}^k_{rd}\hat{\sigma}^j_{dr}\}\right).\end{aligned} \tag{14}$$

In the master equation, we assume that single body decay γ_r is large and the molecular coupling is strong. The even weaker Hamiltonian H will be taken into account adiabatically.

We first focus on the subspace expanded by the two Rydberg states. Due to the strong single body decay, the system rapidly reaches the equilibrium state. To consider different time scales, the master equation $\dot{\hat{\rho}} = (\mathcal{L}_0 + \mathcal{L}_1)\hat{\rho}$ is split into the fast (denoted by $\mathcal{L}_0\hat{\rho}$) and slow (denoted by $\mathcal{L}_1\hat{\rho}$) parts, where

$$\begin{aligned}\frac{\mathcal{L}_0\hat{\rho}}{\gamma_r} &= \sum_{j,k=1,2,j\neq k} \left(\hat{\sigma}^j_{dr}\hat{\rho}_m\hat{\sigma}^k_{rd} - \frac{1}{2}\{\hat{\rho}_m, \hat{\sigma}^k_{rd}\hat{\sigma}^j_{dr}\}\right), \\ \mathcal{L}_1\hat{\rho} &= -i[\hat{H}_m, \hat{\rho}_m].\end{aligned} \tag{15}$$

We will trace the fast dynamics and derive an effective master equation for the slow dynamics via the second order perturbation calculation [67].

Here we define a projection operator $\mathcal{P}_0 = \lim_{t\to\infty} e^{t\mathcal{L}_0}$, which projects the density matrix to the subspace corresponding to the relatively slow dynamics, i.e. $\hat{\rho} = \mathcal{P}_0\hat{\rho}_m$. The first order correction vanishes $\mathcal{P}_0\mathcal{L}_1\mathcal{P}_0\hat{\rho}_m = 0$. We then calculate the second order correction $-\mathcal{P}_0\mathcal{L}_1(\mathcal{I} - \mathcal{P}_0)\mathcal{L}_1\mathcal{P}_0\hat{\rho}_m$.

Optics EXPRESS

A tedious but straightforward calculation yields an effective master equation depending on the two-atom dephasing,

$$\dot{\hat{\rho}}_e \approx \frac{2U^2(R_{12})}{\gamma_r}\left(\hat{\sigma}^1_{dd}\hat{\sigma}^2_{dd}\hat{\rho}_e\hat{\sigma}^2_{dd}\hat{\sigma}^1_{dd} - \frac{1}{2}\{\hat{\sigma}^2_{dd}\hat{\sigma}^1_{dd}, \hat{\rho}_e\}\right). \tag{16}$$

Defining $\Gamma_{12} = 2U^2(R_{12})/\gamma_r$ and taking Hamiltonian H and other process into account adiabatically, we obtain the master equation given in the main text (by further extending the approximate result to the many-atom setting).

Funding

Ministry of Education of the People's Republic of China (2014AA014402, Z2017030); National Natural Science Foundation of China (11204019, 11847221, 11874004, 11904104); Education Department of Jilin Province (JJKH20200557KJ); China Scholarship Council (201707535012); China Postdoctoral Science Foundation (2017M620140); Engineering and Physical Sciences Research Council (EP/M014266/1, EP/R04340X/1); Chinese Service Center for Scholarly Exchange (20180040); UK-India Education and Research Initiative (IND/CONT/G/16-17/73); University of Nottingham.

Disclosures

The authors declare no conflicts of interest.

References

1. S. E. Harris, J. E. Field, and A. Imamoglu, "Nonlinear optical processes using electromagnetically induced transparency," Phys. Rev. Lett. **64**(10), 1107–1110 (1990).
2. K.-J. Boller, A. Imamoglu, and S. E. Harris, "Observation of electromagnetically induced transparency," Phys. Rev. Lett. **66**(20), 2593–2596 (1991).
3. M. Fleischhauer, A. Imamoglu, and J. P. Marangos, "Electromagnetically induced transparency: Optics in coherent media," Rev. Mod. Phys. **77**(2), 633–673 (2005).
4. C. Liu, Z. Dutton, C. H. Behroozi, and L. V. Hau, "Observation of coherent optical information storage in an atomic medium using halted light pulses," Nature (London) **409**(6819), 490–493 (2001).
5. M. D. Lukin, "*Colloquium*: Trapping and manipulating photon states in atomic ensembles," Rev. Mod. Phys. **75**(2), 457–472 (2003).
6. T. Chaneliere, D. N. Matsukevich, S. D. Jenkins, S.-Y. Lan, T. A. B. Kennedy, and A. Kuzmich, "Storage and retrieval of single photons transmitted between remote quantum memories," Nature (London) **438**(7069), 833–836 (2005).
7. J. Appel, E. Figueroa, D. Korystov, M. Lobino, and A. I. Lvovsky, "Quantum Memory for Squeezed Light," Phys. Rev. Lett. **100**(9), 093602 (2008).
8. A. I. Lvovsky, B. C. Sanders, and W. Tittel, "Optical quantum memory," Nat. Photonics **3**(12), 706–714 (2009).
9. M. Paternostro, M. S. Kim, and B. S. Ham, "Generation of entangled coherent states via cross-phase-modulation in a double electromagnetically induced transparency regime," Phys. Rev. A **67**(2), 023811 (2003).
10. M. G. Payne and L. Deng, "Quantum Entanglement of Fock States with Perfectly Efficient Ultraslow Single-Probe Photon Four-Wave Mixing," Phys. Rev. Lett. **91**(12), 123602 (2003).
11. C. Ottaviani, D. Vitali, M. Artoni, F. Cataliotti, and P. Tombesi, "Polarization Qubit Phase Gate in Driven Atomic Media," Phys. Rev. Lett. **90**(19), 197902 (2003).
12. D. Petrosyan, "Towards deterministic optical quantum computation with coherently driven atomic ensembles," J. Opt. B: Quantum Semiclassical Opt. **7**(7), S141–S151 (2005).
13. A. V. Gorshkov, R. Nath, and T. Pohl, "Dissipative Many-Body Quantum Optics in Rydberg Media," Phys. Rev. Lett. **110**(15), 153601 (2013).
14. O. Firstenberg, C. S. Adams, and S. Hofferber, "Nonlinear quantum optics mediated by Rydberg interactions," J. Phys. B: At., Mol. Opt. Phys. **49**(15), 152003 (2016).
15. Q.-Y. Liang, A. V. Venkatramani, S. H. Cantu, T. L. Nicholson, M. J. Gullans, A. V. Gorshkov, J. D. Thompson, C. Chin, M. D. Lukin, and V. Vuletic, "Observation of three-photon bound states in a quantum nonlinear medium," Science **359**(6377), 783–786 (2018).
16. M. Saffman, T. G. Walker, and K. Mølmer, "Quantum information with Rydberg atoms," Rev. Mod. Phys. **82**(3), 2313–2363 (2010).
17. M. Saffman and T. G. Walker, "Creating single-atom and single-photon sources from entangled atomic ensembles," Phys. Rev. A **66**(6), 065403 (2002).

Optics EXPRESS

18. T. G. Walker, "Strongly interacting photons," Nature **488**(7409), 39–40 (2012).
19. M. M. Müller, A. Kölle, R. Löw, T. Pfau, T. Calarco, and S. Montangero, "Room-temperature Rydberg single-photon source," Phys. Rev. A **87**(5), 053412 (2013).
20. T. Peyronel, O. Firstenberg, Q.-Y. Liang, S. Hofferberth, A. V. Gorshkov, T. Pohl, M. D. Lukin, and V. Vuletic, "Quantum nonlinear optics with single photons enabled by strongly interacting atoms," Nature (London) **488**(7409), 57–60 (2012).
21. J. Honer, R. Löw, H. Weimer, T. Pfau, and H. P. Bü chler, "Artificial Atoms Can Do More Than Atoms: Deterministic Single Photon Subtraction from Arbitrary Light Fields," Phys. Rev. Lett. **107**(9), 093601 (2011).
22. A. V. Gorshkov, J. Otterbach, M. Fleischhauer, T. Pohl, and M. D. Lukin, "Photon-Photon Interactions via Rydberg Blockade," Phys. Rev. Lett. **107**(13), 133602 (2011).
23. H. Gorniaczyk, C. Tresp, J. Schmidt, H. Fedder, and S. Hofferberth, "Single-Photon Transistor Mediated by Interstate Rydberg Interactions," Phys. Rev. Lett. **113**(5), 053601 (2014).
24. D. Tiarks, S. Baur, K. Schneider, S. Dürr, and G. Rempe, "Single-Photon Transistor Using a Förster Resonance," Phys. Rev. Lett. **113**(5), 053602 (2014).
25. W. Chen, K. M. Beck, R Bücker, M. Gullans, M. D. Lukin, H. Tanji-Suzuki, and V. Vuletić, "All-Optical Switch and Transistor Gated by One Stored Photon," Science **341**(6147), 768–770 (2013).
26. S. Baur, D. Tiarks, G. Rempe, and S. Dürr, "Single-Photon Switch Based on Rydberg Blockade," Phys. Rev. Lett. **112**(7), 073901 (2014).
27. I. Friedler, G. Kurizki, and D. Petrosyan, "Deterministic quantum logic with photons via optically induced photonic band gaps," Phys. Rev. A **71**(2), 023803 (2005).
28. D. Paredes-Barato and C. S. Adams, "All-Optical Quantum Information Processing Using Rydberg Gates," Phys. Rev. Lett. **112**(4), 040501 (2014).
29. M. O. Scully and M. S. Zubairy, *Quantum Optics* (Cambridge University Press, Cambridge, England, 1997).
30. I. Lesanovsky and J. P. Garrahan, "Kinetic Constraints, Hierarchical Relaxation, and Onset of Glassiness in Strongly Interacting and Dissipative Rydberg Gases," Phys. Rev. Lett. **111**(21), 215305 (2013).
31. K. Macieszczak, Y. L. Zhou, S. Hofferberth, J. P. Garrahan, W. Li, and I. Lesanovsky, "Metastable decoherence-free subspaces and electromagnetically induced transparency in interacting many-body systems," Phys. Rev. A **96**(4), 043860 (2017).
32. F. Letscher, O. Thomas, T. Niederprüm, M. Fleischhauer, and H. Ott, "Bistability Versus Metastability in Driven Dissipative Rydberg Gases," Phys. Rev. X **7**(2), 021020 (2017).
33. S. Ray, S. Sinha, and K. Sengupta, "Phases, collective modes, and nonequilibrium dynamics of dissipative Rydberg atoms," Phys. Rev. A **93**(3), 033627 (2016).
34. M. Hoening, W. Abdussalam, M. Fleischhauer, and T. Pohl, "Antiferromagnetic long-range order in dissipative Rydberg lattices," Phys. Rev. A **90**(2), 021603 (2014).
35. D. W. Schönleber, M. Gärttner, and J. Evers, "Coherent versus incoherent excitation dynamics in dissipative many-body Rydberg systems," Phys. Rev. A **89**(3), 033421 (2014).
36. J. T. Young, T. Boulier, E. Magnan, E. A. Goldschmidt, R. M. Wilson, S. L. Rolston, J. V. Porto, and A. V. Gorshkov, "Dissipation-induced dipole blockade and antiblockade in driven Rydberg systems," Phys. Rev. A **97**(2), 023424 (2018).
37. Z. Ficeka and R. Tanaś, "Entangled states and collective nonclassical effects in two-atom systems," Phys. Rep. **372**(5), 369–443 (2002).
38. B. P. Venkatesh, M. L. Juan, and O. Romero-Isart, "Cooperative Effects in Closely Packed Quantum Emitters with Collective Dephasing," Phys. Rev. Lett. **120**(3), 033602 (2018).
39. T. G. Walker and M. Saffman, "Zeros of Rydberg–Rydberg Föster interactions," J. Phys. B **38**(2), S309–S319 (2005).
40. T. G. Walker and M. Saffman, "Consequences of Zeeman degeneracy for the van der Waals blockade between Rydberg atoms," Phys. Rev. A **77**(3), 032723 (2008).
41. J. Nipper, J. B. Balewski, A. T. Krupp, B. Butscher, R. Löw, and T. Pfau, "Highly Resolved Measurements of Stark-Tuned Förster Resonances between Rydberg Atoms," Phys. Rev. Lett. **108**(11), 113001 (2012).
42. S. Ravets, H. Labuhn, D. Barredo, L. Beguin, T. Lahaye, and A. Browaeys, "Coherent dipole–dipole coupling between two single Rydberg atoms at an electrically-tuned Förster resonance," Nat. Phys. **10**(12), 914–917 (2014).
43. Browaeys Antoine, Barredo Daniel, and Lahaye Thierry, "Experimental investigations of dipole–dipole interactions between a few Rydberg atoms," J. Phys. B **49**(15), 152001 (2016).
44. Paris-Mandoki Asaf, Gorniaczyk Hannes, Tresp Christoph, Mirgorodskiy Ivan, and Hofferberth Sebastian, "Tailoring Rydberg interactions via Förster resonances: state combinations, hopping and angular dependence," J. Phys. B **49**(16), 164001 (2016).
45. H. Gorniaczyk, C. Tresp, P. Bienias, A. Paris-Mandoki, W. Li, I. Mirgorodskiy, H. P. Büchler, I. Lesanovsky, and S. Hofferberth, "Enhancement of Rydberg-mediated single-photon nonlinearities by electrically tuned Förster resonances," Nat. Commun. **7**(1), 12480 (2016).
46. C. Tresp, P. Bienias, S. Web er, H. Gorniaczyk, I. Mirgorodskiy, H. P. Büchler, and S. Hofferberth, "Dipolar Dephasing of Rydberg *D*-State Polaritons," Phys. Rev. Lett. **115**(8), 083602 (2015).
47. R. Boddeda, I. Usmani, E. Bimbard, A. Grankin, A. Ourjoumtsev, E. Brion, and P. Grangier, "Rydberg-induced optical nonlinearities from a cold atomic ensemble trapped inside a cavity," J. Phys. B: At., Mol. Opt. Phys. **49**(8), 084005 (2016).

Optics EXPRESS

48. W. Li, D. Viscor, S. Hofferberth, and I. Lesanovsky, "Electromagnetically Induced Transparency in an Entangled Medium," Phys. Rev. Lett. **112**(24), 243601 (2014).
49. D. Cano and J. Fortagh, "Multiatom entanglement in cold Rydberg mixtures," Phys. Rev. A **89**(4), 043413 (2014).
50. Y.-M. Liu, X.-D. Tian, D. Yan, Y. Zhang, C.-L. Cui, and J.-H. Wu, "Nonlinear modifications of photon correlations via controlled single and double Rydberg blockade," Phys. Rev. A **91**(4), 043802 (2015).
51. X.-R. Huang, Z.-X. Ding, C.-S. Hu, L.-T. Shen, W. B. Li, H. Z. Wu, and S.-B. Zheng, "Robust Rydberg gate via Landau-Zener control of Förster resonance," Phys. Rev. A **98**(5), 052324 (2018).
52. D. Viscor, W. Li, and I. Lesanovsky, "Electromagnetically induced transparency of a single-photon in dipole-coupled one-dimensional atomic clouds," New J. Phys. **17**(3), 033007 (2015).
53. D. Petrosyan, J. Otterbach, and M. Fleischhauer, "Electromagnetically Induced Transparency with Rydberg Atoms," Phys. Rev. Lett. **107**(21), 213601 (2011).
54. K. J. Weatherill, J. D. Pritchard, R. P. Abel, M. G. Bason, A. K. Mohapatra, and C. S. Adams, "Electromagnetically induced transparency of an interacting cold Rydberg ensemble," J. Phys. B: At., Mol. Opt. Phys. **41**(20), 201002 (2008).
55. J. D. Pritchard, D. Maxwell, A. Gauguet, K. J. Weatherill, M. P. A. Jones, and C. S. Adams, "Cooperative Atom-Light Interaction in a Blockaded Rydberg Ensemble," Phys. Rev. Lett. **105**(19), 193603 (2010).
56. J. D. Pritchard, A. Gauguet, K. J. Weatherill, and C. S. Adams, "Optical non-linearity in a dynamical Rydberg gas," J. Phys. B: At., Mol. Opt. Phys. **44**(18), 184019 (2011).
57. J. Reslen, "Many-body effects in a model of electromagnetically induced transparency," J. Phys. B: At., Mol. Opt. Phys. **44**(19), 195505 (2011).
58. C. Ates, S. Sevinçli, and T. Pohl, "Electromagnetically induced transparency in strongly interacting Rydberg gases," Phys. Rev. A **83**(4), 041802 (2011).
59. D. Yan, Y.-M. Liu, Q.-Q. Bao, C.-B. Fu, and J.-H. Wu, "Electromagnetically induced transparency in an inverted-Y system of interacting cold atoms," Phys. Rev. A **86**(2), 023828 (2012).
60. D. Yan, C.-L. Cui, Y.-M. Liu, L.-J. Song, and J.-H. Wu, "Normal and abnormal nonlinear electromagnetically induced transparency due to dipole blockade of Rydberg excitation," Phys. Rev. A **87**(2), 023827 (2013).
61. H. H. Jen and Daw-Wei Wang, "Theory of electromagnetically induced transparency in strongly correlated quantum gases," Phys. Rev. A **87**(6), 061802 (2013).
62. M. Gärttner and J. Evers, "Nonlinear absorption and density-dependent dephasing in Rydberg electromagnetically-induced-transparency media," Phys. Rev. A **88**(3), 033417 (2013).
63. J. Stanojevic, V. Parigi, E. Bimbard, A. Ourjoumtsev, and P. Grangier, "Dispersive optical nonlinearities in a Rydberg electromagnetically-induced-transparency medium," Phys. Rev. A **88**(5), 053845 (2013).
64. Y.-M. Liu, D. Yan, X.-D. Tian, C.-L. Cui, and J.-H. Wu, "Electromagnetically induced transparency with cold Rydberg atoms: Superatom model beyond the weak-probe approximation," Phys. Rev. A **89**(3), 033839 (2014).
65. Y.-M. Liu, X.-D. Tian, X. Wang, D. Yan, and J.-H. Wu, "Cooperative nonlinear grating sensitive to light intensity and photon correlation," Opt. Lett. **41**(2), 408 (2016).
66. O. Firstenberg, T. Peyronel, Q.-Y. Liang, A. V. Gorshkov, M. D. Lukin, and V. Vuletić, "Attractive photons in a quantum nonlinear medium," Nature (London) **502**(7469), 71–75 (2013).
67. C. Gardiner and P. Zoller, *Quantum Noise* (Springer, 2004).